Epitaxial growth of MgO nanowires by pulsed laser deposition

Kazuki Nagashima, Takeshi Yanagida,[a] Hidekazu Tanaka, and Tomoji Kawai
Institute of Scientific and Industrial Research, Osaka University, 8-1 Mihogaoka, Ibaraki, Osaka 567-0047, Japan

(Received 24 January 2007; accepted 4 May 2007; published online 21 June 2007)

We fabricated single-crystalline MgO nanowires epitaxially grown on MgO single crystal substrate using the Au catalyst-assisted pulsed laser deposition (PLD). Controlling appropriately the amount of Au catalyst and the substrate temperature was found to be crucial for the MgO nanowire growth using the catalyst-assisted PLD. In addition, (100) oriented MgO nanowires were epitaxially grown on (100), (110), and (111) oriented substrates, allowing the limited growth directions. The possible growth mechanism of MgO nanowires in PLD is discussed. This feasibility of PLD for fabricating MgO nanowires would contribute to incorporating the rich functionalities of various transition metal oxides into nanowires via *in situ* construction of heterostructures in oxide nanowires. © *2007 American Institute of Physics*. [DOI: 10.1063/1.2748625]

One-dimensional nanostructures have become attractive and being actively investigated since they are promising nanoscale building blocks for exploring nanoscale devices including electronics,[1–3] photonics,[4,5] and ultrasensitive biomolecule sensors.[6,7] Mainly, conventional semiconductors including silicon and its compounds have been focused on as the nanowire materials. Integrating more functionality into the nanowires by using other functional materials would be fascinating for advanced nanowire devices in the future. For instance, transition metal oxides are well known to exhibit the rich variation of the physical properties, such as superconductivity, ferromagnetism, and ferroelectricity.[8–10] Such rich functionalities of oxide materials might expand the application range of nanowire devices.[11–13] As to the synthesis of oxide materials, pulsed laser deposition (PLD) has been one of the most powerful techniques to fabricate various functional oxide thin films,[14,15] nonequilibrium oxides,[16] and the heterostructures.[17] Since the interface of oxide heterostructures plays a crucial role on the physical properties of thin films,[17,18] *in situ* fabrication of such oxide heterostructures in nanowires is strongly desired to avoid the degradation of oxide interfaces due to the atmospheric exposure. Thus the feasibility of PLD technique to fabricate the diverse oxide nanowires will contribute to the integration of rich oxide functionalities into nanowires via *in situ* construction of oxide heterostructures in nanowires.

Magnesium oxide (MgO) might find potential applications including catalysis, additives in refractory, paint, and insulating layers in tunnel magnetoresistance junctions,[19,20] and herein more importantly as single crystal substrates for transition metal oxide thin film growth due to the small lattice mismatch with many transition metal oxides including magnetite,[21] other spinel ferrites,[22] and perovskite oxides.[23] As such the availability of MgO nanowires using PLD will allow the *in situ* integration of functional oxide materials into the nanowires. MgO nanowires, in fact, have been mainly fabricated by catalysis-assisted chemical-vapor deposition (CVD) technique and other techniques in the literature,[24–28] although the feasibility of PLD technique for fabricating oxide nanowires including ZnO, which can be grown even in the absence of a metal catalyst due to the anisotropy of crystal growth, has been demonstrated.[29–31] On the contrary there seem to be no reports concerning with MgO nanowires fabricated by PLD. In addition, the detailed knowledge as to the controllability of MgO nanowire morphologies, including the size and the growth direction, is scarce. Herein we report the fabrication of epitaxially grown MgO nanowires using the Au catalyst-assisted PLD.

MgO nanowires were grown on MgO (100) single crystal substrate by Au catalyst-assisted PLD. Au catalyst was patterned on the 5×5 mm^2 substrate by sputtering with metal mask. The thickness of Au catalyst was controlled from 1 to 10 nm by changing the sputtering time. MgO single crystal was used as a source of Mg species vapor. ArF excimer laser ($\lambda=193$ nm) was used for the laser ablation. The laser energy, the repetition rate, and the oxygen pressure were set to be 40 mJ, 10 Hz, and 1 Pa, respectively. The substrate temperature for growth was varied from 400 to 800 °C. The typical background pressure was 10^{-4} Pa. Prior to the laser ablation, the Au patterned MgO (100) substrate was preheated at the growth temperature for 10 min. The substrate was placed 30 mm away from the target. The laser ablation was performed for 60 min. Subsequently the samples were cooled down to room temperature in 30 min. The nanowire morphology was characterized by field emission scanning electron microscopy (FESEM) (JEOL JSM-6330FT). High-resolution transmission electron microscopy (TEM) (JEOL JEM-3000F) coupled with energy dispersive spectroscopy (EDS) was used to evaluate the diameter, the crystallinity, and the composition of the fabricated nanowires. Samples for TEM were prepared by placing a drop of the sample suspension on a copper microgrid (JEOL 7801-11613). TEM measurements were performed at the accelerating voltage of 300 kV. The crystal structure of the as-synthesized products was analyzed by x-ray diffraction (XRD).

[a]Electronic mail: yanagi32@sanken.osaka-u.ac.jp

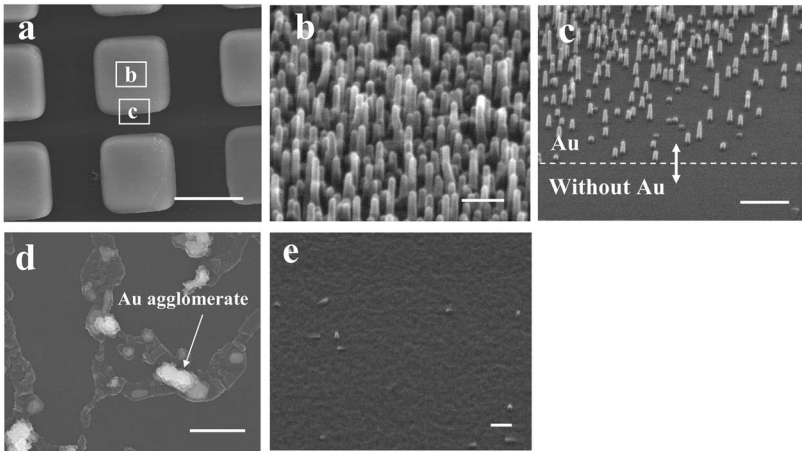

FIG. 1. FESEM images of MgO nanowires on MgO (100) single crystal substrate. In images (a), (b), and (c), the nanowires were grown under 800 °C substrate temperature and 1 nm Au film thickness. (a) Patterned area of Au on MgO (100) single crystal substrate. The scale bar is 500 μm. (b) Morphologies of MgO nanowires in central area "b" in (a). The scale bar is 100 nm. (c) Morphologies of MgO nanowires in boundary area "c" in (a). The scale bar is 100 nm. (d) Effect of the amount of Au catalyst on the morphologies of deposited surface. The Au catalyst thickness was 10 nm and the substrate temperature was 800 °C. The scale bar is 1 μm. (e) Dependence of the substrate temperature on the morphologies of deposited surface. The substrate temperature was 400 °C and the Au catalyst thickness was 1 nm. The scale bar is 100 nm.

Figure 1 shows the typical FESEM images of the sample morphology. The growths were performed under 800 °C substrate temperature and 1 nm Au film thickness. The Au patterned area on the MgO substrate can be seen in Fig. 1(a). The magnified image near the center of the pattered area is shown in Fig. 1(b). Nanowire structures were clearly observed, and the size was found to be relatively homogeneous in the image. The magnified image near the boundary of the patterned area is shown in Fig. 1(c). It can be seen that the nanowires were only grown for Au patterned area, indicating the important role of Au catalyst on the nanowire growth. In addition, most nanowires were grown perpendicular to the substrate, inferring the epitaxial growth of nanowires. The average nanowire length grown for 60 min was 150 nm. It is noted that the appearance of MgO nanowires is sensitive to several experimental conditions. For instance, when varying the thickness of Au catalyst from 1 up to 10 nm, the presence of nanowires has not been observed at all above 5 nm, as shown in Fig. 1(d), in which Au agglomerates only were observed. Such critical dependence on the nanowire growth was also found for the variation of the substrate temperature. Figure 1(e) shows the image when the substrate temperature was set to be below 450 °C. Clearly there were no observable nanowires due to such lower substrate temperature. Thus it is crucial to control appropriately the ambient conditions, including mainly the amount of Au catalyst and the substrate temperature, for the nanowire growth using PLD. Figure 2(a) shows the 2θ-θ scan data of XRD for MgO nanowires grown on MgO (100) single crystal substrate under 800 °C substrate temperature and 1 nm Au film thickness. Only one diffraction peak corresponding to the MgO (200) plane was detected, indicating the epitaxy of MgO nanowire growth on MgO (100) single crystal substrate. Figure 2(b) shows the nanowire length versus the growth time for nanowires grown under 800 °C substrate temperature and 1 nm Au film thickness. It can be seen that the nanowire length increases with increasing growth time within the investigated time scale. Although the average diameter of nanowires was approximately 15–20 nm in the FESEM images, the values are overestimated due to the use of platinum coating that prevents charging in SEM measurements. high-resolution TEM (HRTEM)-EDS analysis was performed to obtain more detailed information in the context of the nanowires, such as the exact size, the crystallinity, and the composition. Figure 3(a) shows the HRTEM image of the MgO nanowires. The presence of the catalyst droplet on the wire tip can be clearly seen in the image. As to the crystallinity of the nanowires, the lattice fringes of nanowires were observed in the HRTEM image, as shown in the inset figure. It reveals that the spacing of 0.21 nm between adjacent lattice planes corresponds to the distance between (200) crystal planes of MgO, indicating the single crystal nature of the MgO nanowires. In addition, the selected area electron diffraction (SAED) pattern of the MgO nanowire reveals that the nearest diffraction spot to the center corresponds to the (200) plane, as shown in Fig. 3(c). To confirm the compositions of both droplets and wires, EDS analysis was performed at each area, as shown in Figs. 3(d) and 3(e). Cu signals in these EDS spectra are originated from the TEM grids. The droplets are mainly composed of Au, and the wires are formed by Mg and O with

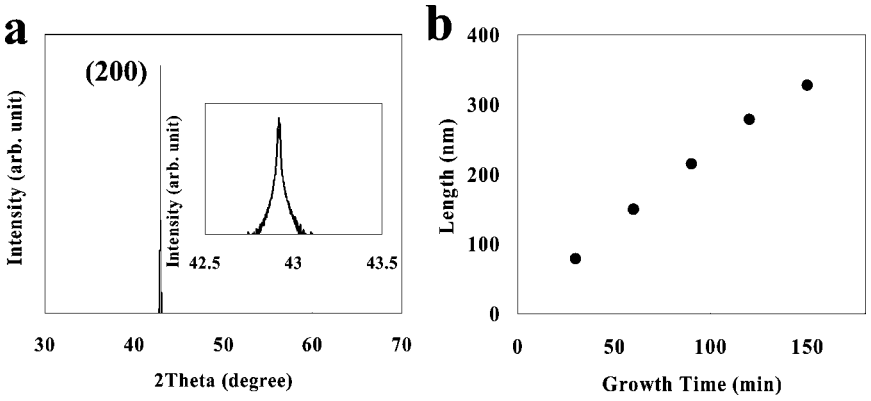

FIG. 2. XRD data of MgO nanowires grown on (100) substrate and the nanowire length vs the growth time. The nanowires were grown under 800 °C substrate temperature and 1 nm Au film thickness. (a) XRD data of MgO nanowires grown on (100) substrate. The inset shows the zoom-in view of the primary peak at (200) plane. (b) Growth time dependence on nanowire length.

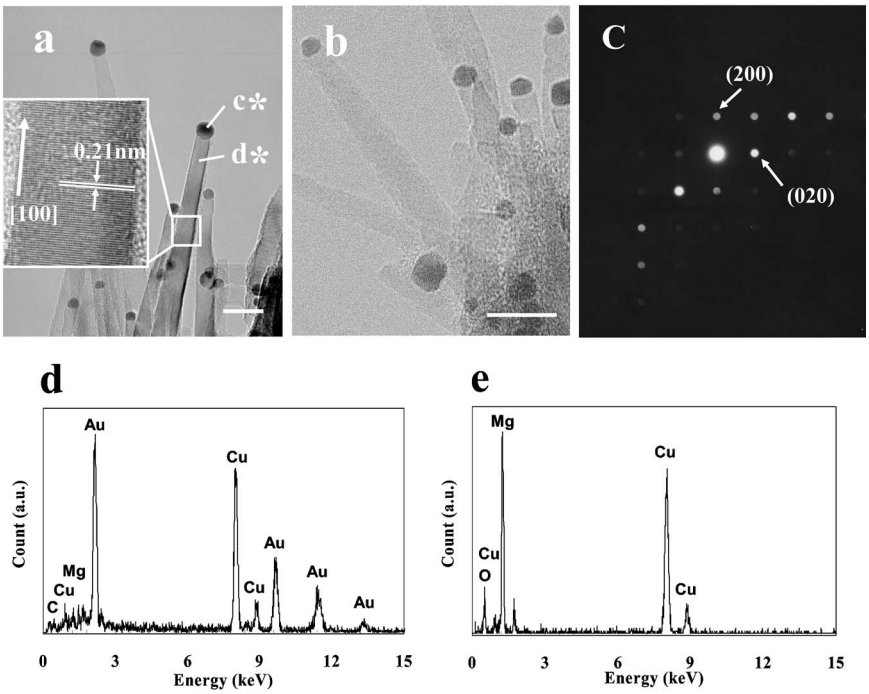

FIG. 3. HRTEM images of MgO nanowires and the EDS data. The nanowires were grown under 800 °C substrate temperature and 1 nm Au film thickness. (a) HRTEM image of MgO nanowires. The scale bar is 20 nm. The inset figure shows the lattice fringe image. (b) HRTEM image of small MgO nanowires. The scale bar is 5 nm. (c) SAED pattern of MgO nanowires. (d) EDS data at "c*" position in (a). (e) EDS data at "d*" position in (a).

the ratio of Mg to O approximately equal to 1:1. In addition, as can be seen in Fig. 3(b), the average diameter size could be controlled down to 3–5 nm by manipulating the Au droplet size. The preferential [100] growth observed in MgO nanowires might be principally extended to control the growth direction from the substrate. Figure 4 shows the orientation effect of MgO substrate on the growth direction of MgO nanowires using MgO (100), (110), and (111) oriented single crystal substrates. Figures 4(a) and 4(b) show the tilted FESEM images for (100) and (110) substrates, respectively, and Fig. 4(c) shows the top-view image of (111) substrate. The growth direction of fabricated nanowires strongly depends on the substrate orientation. Clearly, the epitaxial growth of MgO nanowires along the [100] direction limits the growth direction of nanowires for each oriented substrate. Note that nanowires more than 90% follow the growth regime. In addition, such epitaxitial growths of [100] oriented MgO nanowires grown on (110) and (111) substrates were also confirmed by XRD measurements, as shown in Figs. 4(d) and 4(e). Considering the experimental results including the presence of catalyst on the wire tip, the vapor-liquid-solid (VLS) mechanism seems to be responsible for the MgO nanowire growth in PLD.[32] Within the framework of the VLS mechanism,[33] a supersaturation is an important process for the nanowire growth. When varying the amount of catalyst and the substrate temperature, the degree of supersaturation within the catalyst might be altered. In addition, the diffused adatoms on the substrate surface rather than impinging species play an important role on the VLS growth.[34] These might explain why the MgO nanowires can

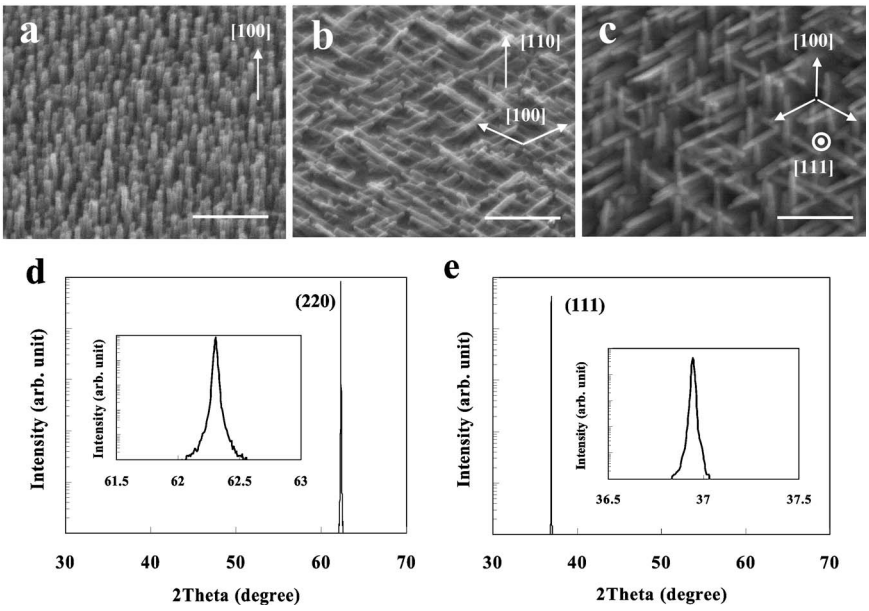

FIG. 4. Orientation effect of MgO substrate on the growth direction of MgO nanowires. The nanowires were grown under 800 °C substrate temperature and 1 nm Au film thickness. (a) Tilted image of MgO nanowires grown on (100) substrate. (b) Tilted image of MgO nanowires grown on (110) substrate. (c) Top-view image of MgO nanowires grown on (111) substrate. (d) XRD data of MgO nanowires grown on (110) substrate. The inset shows the zoom-in view of the primary peak at (220) plane. (e) XRD data of MgO nanowires grown on (111) substrate. The inset shows the zoom-in view of the primary peak at (111) plane.

be grown in catalyst-assisted PLD, and the critical dependencies on the nanowire growth exist when varying the amount of catalyst and the substrate temperature. For example, increasing catalyst thickness results in increasing catalyst droplet size.[35] If the diffusion length of adatoms is solely dependent on the substrate temperature at constant ambient pressure, the diffusion flux of adatoms into the individual catalyst droplet is enhanced with decreasing the droplet size at constant substrate temperature, which varies the degree of supersaturation within the catalyst droplet. This might explain the crucial dependence of the amount of catalyst on the MgO nanowire growth in terms of the variation of supersaturation. As to the substrate temperature effects, there are two possible factors affecting the MgO nanowire growth. One is related to the phenomenon of melting Au catalyst, since the melting temperature of Au bulk is 1064 °C, which is much higher than the substrate temperature used. Clearly decreasing the substrate temperature prevents the melting of Au catalyst, which strongly affects the VLS growth via the absence of liquid phase. The other factor might be the diffusion flux of adatoms. Since increasing the substrate temperature enhances the surface diffusion of adatoms, the diffusion flux into the catalyst droplet decreases with decreasing the substrate temperature. This also varies the degree of supersaturation within the droplet. Although the present understanding of the MgO nanowire growth is not comprehensive, above qualitative interpretations would contribute to the further understanding of oxide nanowire growth in PLD and also controlling oxide nanowire morphologies.

In conclusion, we have fabricated epitaxially grown MgO nanowires using Au catalyst-assisted PLD technique. As to the properties of MgO nanowires, the well-crystallized structures, the average size down to 5 nm, and the stoichiometry were confirmed by HRTEM-EDS. The preferential epitaxial growth of [100] direction could be extended to control the growth direction of nanowires by varying the substrate orientation. The feasibility of PLD technique for fabricating MgO nanowires will allow the integration of rich functionalities of many transition metal oxides into oxide nanowires via *in situ* fabrication of oxide heterostructures.

ACKNOWLEDGMENTS

The authors would like to thank the Ministry of Education, Culture, Sports, Science and Technology of Japan for funding and supporting this project though the Center of Excellence (COE) Program. The authors also acknowledge M. Kanai for constructive advices and T. Ishibashi for his invaluable technical support. One of the authors (K.N.) greatly thanks the Micron Technology for scholarship.

[1] F. Patolsky, B. D. Timko, G. Yu, Y. Fang, A. B. Greytak, G. Zheng, and C. M. Lieber, Science **313**, 1100 (2006).
[2] J. Xiang, W. Lu, Y. Hu, Y. Wu, H. Yan, and C. M. Lieber, Nature (London) **441**, 489 (2006).
[3] R. S. Friedman, M. C. McAlpine, D. S. Ricketts, D. Ham, and C. M. Lieber, Nature (London) **434**, 1085 (2005).
[4] O. Hayden, R. Agarwal, and C. M. Lieber, Nat. Mater. **5**, 352 (2006).
[5] C. J. Barrelet, J. Bao, M. Lončar, H. G. Park, F. Capasso, and C. M. Lieber, Nano Lett. **6**, 11 (2006).
[6] F. Patolsky, G. Zheng, and C. M. Lieber, Anal. Chem. **78**, 4260 (2006).
[7] G. Zheng, F. Patolsky, Y. Cui, W. U. Wang, and C. M. Lieber, Nat. Biotechnol. **23**, 1294 (2005).
[8] W. Ramadan *et al.*, Phys. Rev. B **72**, 205333 (2005).
[9] J. P. Locquet, J. Perret, J. Fompeyrine, E. Mäechler, J. W. Seo, and G. van Tendeloo, Nature (London) **394**, 453 (1998).
[10] B. S. Kwak, A. Erbil, B. J. Wilkens, J. D. Budai, M. F. Chisholm, and L. A. Boatner, Phys. Rev. Lett. **68**, 3733 (1992).
[11] B. Lei, C. Li, D. Zhang, S. Han, and C. Zhou, J. Phys. Chem. B **109**, 18799 (2005).
[12] C. Li, B. Lei, Z. Luo, S. Han, Z. Liu, D. Zhang, and C. Zhou, Adv. Mater. (Weinheim, Ger.) **17**, 1548 (2005).
[13] D. Zhang, Z. Liu, S. Han, C. Li, B. Lei, M. P. Stewart, J. M. Tour, and C. Zhou, Nano Lett. **4**, 2151 (2004).
[14] T. Kanki, T. Yanagida, B. Vilquin, H. Tanaka, and T. Kawai, Phys. Rev. B **71**, 012403 (2005).
[15] T. Yanagida, H. Tanaka, T. Kawai, E. Ikenaga, M. Kobata, J. J. Kim, and K. Kobayashi, Phys. Rev. B **73**, 132503 (2006).
[16] H. Ryoken, N. Ohashi, I. Sakaguchi, Y. Adachi, S. Hishita, and H. Haneda, J. Cryst. Growth **287**, 134 (2006).
[17] T. Kanki, Y. G. Park, H. Tanaka, and T. Kawai, Appl. Phys. Lett. **283**, 4860 (2003).
[18] Y.-G. Park, T. Kanki, H.-Y. Lee, H. Tanaka, and T. Kawai, Solid-State Electron. **47**, 2221 (2003).
[19] H. Tsuji, F. Yagi, H. Hattori, and H. Kita, J. Catal. **148**, 759 (1994).
[20] Y. M. Lee, J. Hayakawa, S. Ikeda, F. Matsukura, and H. Ohno, Appl. Phys. Lett. **89**, 042506 (2006).
[21] D. M. Lind, S. D. Berry, G. Chern, H. Mathias, and L. R. Testardi, Phys. Rev. B **45**, 1838 (1992).
[22] X. ZuO, A. Yang, S. D. Yoon, J. A. Christodoulides, V. G. Harris, and C. Vittoria, J. Appl. Phys. **97**, 10G103 (2005).
[23] I. B. Misirlioglu, S. P. Alpay, F. He, and B. O. Wells, J. Appl. Phys. **99**, 104103 (2006).
[24] H. W. Kim and S. H. Shim, Chem. Phys. Lett. **422**, 165 (2006).
[25] C. Tang, Y. Bando, and T. Sato, J. Phys. Chem. B **106**, 7449 (2002).
[26] Y. Yin, G. Zhang, and Y. Xia, Adv. Funct. Mater. **12**, 293 (2002).
[27] H. Lu, H. Sun, G. Li, C. Chen, D. Yang, and X. Hu, Ceram. Int. **31**, 105 (2005).
[28] X. Wang and D. Xue, Mater. Lett. **60**, 3160 (2006).
[29] T. Nobis, E. M. Kaidashev, A. Rahm, M. Lorenz, J. Lenzner, and M. Grundmann, Nano Lett. **4**, 797 (2004).
[30] M. Lorenz *et al.*, Appl. Phys. Lett. **86**, 143113 (2005).
[31] S. Choopun, H. Tabata, and T. Kawai, J. Cryst. Growth **274**, 167 (2005).
[32] J. Zhan, Y. Bando, J. Hu, and D. Golberg, Inorg. Chem. **43**, 2462 (2004).
[33] J. Hu, T. W. Odom, and C. M. Lieber, Acc. Chem. Res. **32**, 435 (1999).
[34] V. G. Dubrovskii, N. V. Sibirev, G. E. Cirlin, J. C. Harmand, and V. M. Ustinov, Phys. Rev. E **73**, 021603 (2006).
[35] V. G. Dubrovskii, I. P. Soshnikov, G. E. Cirlin, A. A. Tonkikh, Yu. B. Samsonenko, N. V. Sibirev, and V. M. Ustinov, Phys. Status Solidi B **241**, R30 (2004).